L-6

GROWTH AND CONFINEMENT EFFECTS IN III-V SEMICONDUCTOR NANOSTRUCTURES

G. Jolley, Lan Fu, H. H. Tan and C. Jagadish
Department of Electronic Materials Engineering, Research School of Physics and Engineering, The Australian National University, Canberra, ACT, Australia, 0200, Ph. 61 261251590, email gregory.jolley@anu.edu.au

Abstract: *Semiconductor nanostructures have the potential to enhance the performance of numerous opto-electronic devices. Experimental results of quantum dot infrared photodetectors and quantum dot solar cells are presented and the effects of the carrier confinement on the device performance are discussed. Due to the limitation of current quantum dot growth techniques it is concluded that a level of control over the thermal interactions with electrons in nanostructures that would allow these devices to reach their full theoretical potential has not yet been achieved.*

1. Introduction

Semiconductor nanostructures have been utilized in the development of opto-electronic devices with performance characteristics far superior to similar devices constructed from bulk material. For example, semiconductor lasers operate at room temperature with low threshold currents and high efficiencies due to the incorporation of quantum wells (QWs) [1,2]. QW lasers have good performance characteristics predominantly because the quantum confinement alters the density of states in a favourable way such that a greater fraction of the charge carriers have an energy close to the bandgap and lasing wavelength[2]. A larger density of carriers close to the band edges results in a higher optical gain and therefore higher efficiencies and lower threshold currents. It must be noted that the improvements that QW lasers exhibit can be ascribed to the thermal energy distribution of charge carriers in the QW, rather than their dynamics. Nanostructures also have the potential to improve device performance by dramatically altering carrier dynamics. The dark current noise of QW infrared photodetectors (QWIPs) is fundamentally limited by the thermionic emission of electrons from the QWs due to a strong electron-phonon interaction. Quantum dots (QDs) confine charge carriers in all 3-dimensions which results in a discrete density of states. If the energy spacing is different from the phonon energy then a much weaker electron-phonon interaction can lead to smaller dark currents in QD IR photodetectors (QDIPs) and therefore a greater dark current limited detectivity and higher operating temperatures [3]. Essentially, a higher optical to thermal excitation rate should be observed for QD electrons. QDs are also actively being studied in solar cell devices. Theoretical studies conclude that QD solar cells (QDSCs) can potentially achieve efficiencies as high as 63.2%, compared with 40.7% for a single junction GaAs cell, under full concentration [4]. Central to such theoretical predictions is the assumption that carriers in QD states are thermally decoupled from the GaAs barrier states. In this work QDIP and QD solar cell (QDSC) device results are presented and the effects of the carrier confinement on the device performance are discussed.

2. Experimental details

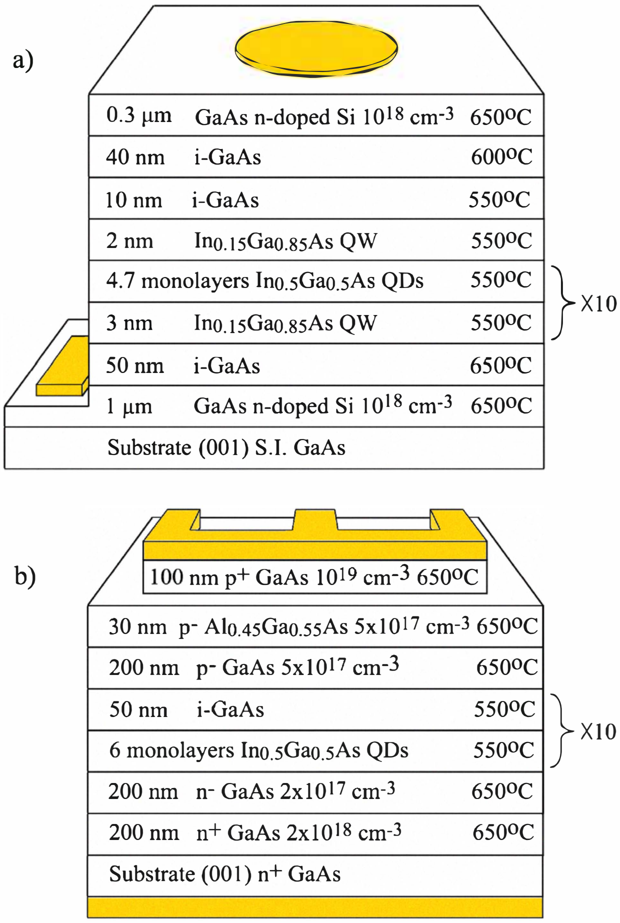

Fig. 1. a) the quantum dot infrared photodetector and b) quantum dot solar cell structures grown by metal-organic chemical vapor deposition. Indicated are the growth temperatures and doping concentrations of the various layers.

QDs for opto-electronic applications are usually always grown by a self-assembled epitaxial method. Depositing thin layers of a semiconductor material with a larger lattice constant onto a substrate results in strain energy which drives 3-dimensional growth. Popular material systems include In(Ga)As QDs on GaAs substrates and

InAs QDs on InP substrates. Due to the self-assembled nature of the QDs there is limited control over their size and shape. For In(Ga)As/GaAs QDs the base width is typically between 15 – 25 nm and the height is 3 – 8 nm and the QD sheet density is usually reported to be about a few 10^{10} cm^{-2}. In addition, QDs formed by the Stranski-Krastanov growth mode always form on a 1D wetting layer, which essentially has the band structure properties of a thin QW. The QDIP and QDSC device structures as shown in Fig. 1 were grown by metal-organic chemical vapor deposition. For both structures a stack of 10 QD layers each of which is separated by 50 nm of GaAs barrier material are sandwiched between GaAs contact layers. Although the QD layers were unintentionally doped electrons can populate the QDIP QD layers due to a small background doping concentration of approximately 5×10^{15} cm^{-3}. Transmission electron microscopy images of single layers of QDs grown under the same conditions indicate a QD sheet density of 4×10^{10} cm^{-2}. The QDs have a base width of approximately 20 nm and a height of 5 nm. The QDIP and QDSC wafers were processed into 250 μm and 1 mm square mesa devices respectively, using contact UV lithography and wet chemical etching. N-type ohmic contacts were formed by the e-beam evaporation of Ge/Au and p-type contacts were formed by evaporating Ti/Au. The contacts were alloyed at 400°C for 60s.

3. Results and discussion

3.1 Quantum dot infrared photodetectors.

The QDIP results are presented first. Fig. 2 shows the bias dependent 77 K spectral response. A single broad peak with a weak bias dependence tends to indicate that the photo-response is predominantly due to transitions from the QD ground state to a band of unbound GaAs barrier states. The conduction band absorption spectrum of InGaAs/GaAs QDs is well understood

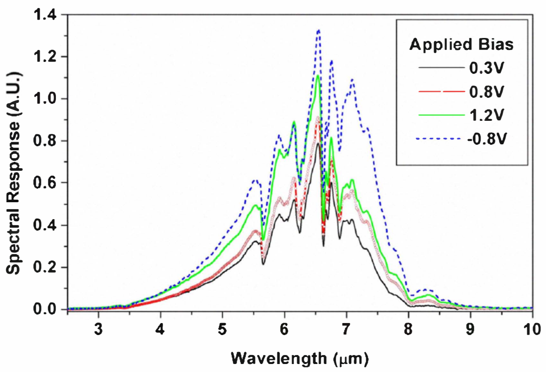

Fig. 2. The 77K normal incidence spectral response of the quantum dot infrared photodetector for various applied biases. The applied bias is with respect to the bottom contact layer.

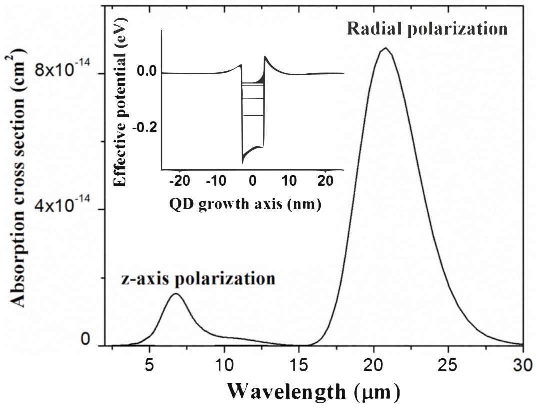

Fig. 3. The calculated optical absorption cross section for light polarized along the QD growth axis and in the radial direction. The QD effective potential as modified by strain and the locations of the first 4 energy levels are shown in the insert.

and is accurately calculated using multiband k·p [5] or single band effective mass models [6]. A single band effective mass calculation of the conduction band absorption spectrum is shown in Fig. 3. The insert of Fig. 3 is the conduction band effective potential as modified by the QD hydrostatic strain. Since the QD base width is significantly larger than the height the absorption spectrum for light that is polarized in the QD growth (z-axis) direction is very different for light that is polarized in the radial direction. In general, radially polarized light induces transitions to energy levels that are significantly bound to the QD which prevents carrier escape. Therefore the measured QDIP photo-response spectrum can be attributed to optical transitions that are induced by light with an electric field in the QD growth direction. There is a good correspondence between the experimental and theoretical absorption spectrum. The QD integrated absorption cross-section strength is limited and given

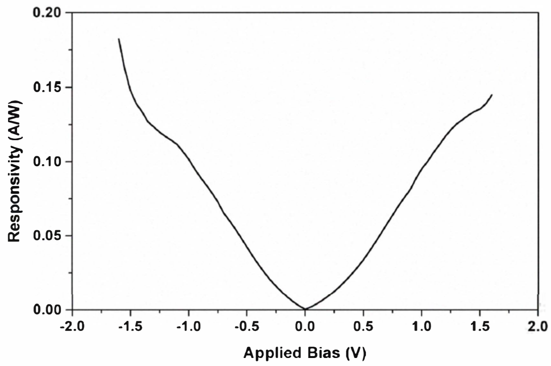

Fig. 4. The QDIP normal incidence 77K integrated responsivity as a function of bias.

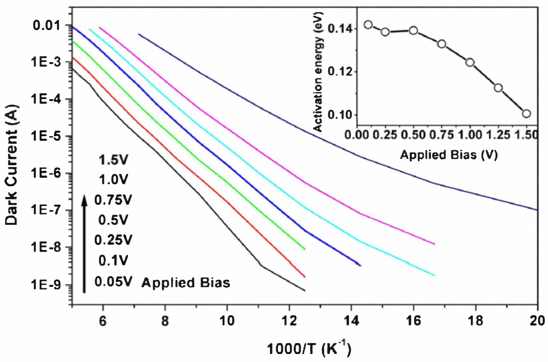

Fig. 5. The QDIP temperature dependent dark current. The insert is the dark current thermal activation energy as a function of bias for the 110-130 K temperature region.

the relatively small QD density that is typically obtained by self-assembled growth, only a small fraction (~ 1%) of the IR light is absorbed by the 10 layers of QDs. This tends to result in modest responsivities which is confirmed by the integrated responsivity plot of Fig. 4. As mentioned, the absorption spectrum of QDs and the effects limiting the absorption strength are well understood. The dark current characteristics of QDs are much less well understood. Fig. 5 displays the temperature dependent dark current and the dark current thermal activation energy. The magnitude of the thermal activation energy and its bias dependence indicates that the dark current is the result of the thermal ejection of electrons from the ground state to the GaAs barrier. Therefore the QDs have a high optical quality since electron tunnelling from QD confined states would result in a significantly smaller thermal activation energy. As is consistent with other reports, the ratio of QDIP photo-response to the dark current is similar or smaller than QWIPs operating at similar wavelengths.

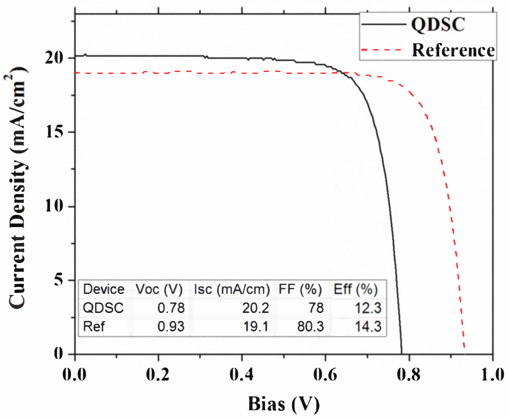

Fig. 6. The light IV curves of the QD and reference solar cells obtained under standard AM 1.5 G conditions. The insert table is the associated device parameters.

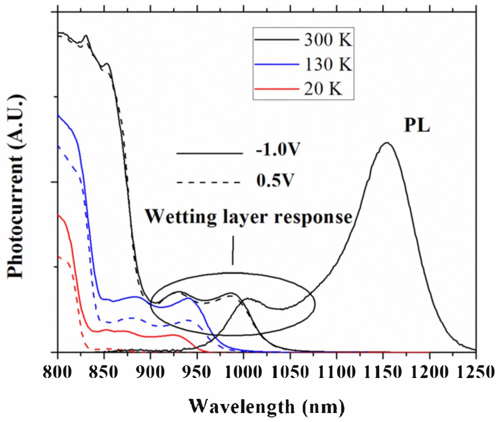

Fig. 7. The spectral response curves of the QDSC for various temperatures and an applied bias of -1.0 and 0.5 V. The photoluminescence curve (PL) is also shown.

There are a number of possible reasons why QDIPs tend to have larger dark currents than what has been theoretically predicted. Ideally, a QD would support a ground state energy level and only a single, degenerate excited state with an energy close to the barrier bandedge. Real QDs have numerous energy levels and a band of WL energy levels that electrons can occupy. In general, the QD ground state and the 1st excited state have a relatively large (~50 meV) energy separation. All other energy levels from the 1st excited state, up to the band of WL states have a much closer energy separation. Therefore the electron-phonon interaction of real QDs is only expected to be weak for transitions between the ground and 1st excited state. Although the rate at which electrons are excited from the ground state could be reduced, subsequent thermal transitions to higher excited states would occur efficiently. Provided electrons in the QD ground state can maintain a thermal equilibrium distribution with excited state electrons a reduction of excitation rate of a ground state electron would not necessarily result in a reduction of the device dark current since electrons in excited states are available for thermionic emission. Since under thermal equilibrium conditions there are far more electrons in the ground state than any excited state a reduction of the thermal interaction with the ground state electrons can still maintain a thermal population of the excited states. These conditions can contribute to the fact that there are no clear indications suggesting that QDIPs have outperformed their QWIP counterparts [7]. Research has been done to develop growth strategies that produce QDs with better engineered bandstructures[8].

3.2 Quantum dot solar cells.

The QDSC with a structure as shown in Fig. 1 b) and a reference single junction GaAs cell in which the QD layers are replaced with 500 nm of GaAs are compared. Light-IV curves obtained under standard AM 1.5 G conditions are shown in Fig. 6. The associated electrical parameters are displayed in the insert table. Consistent with other reports, the incorporation of the QDs increases the short-circuit current while reducing the solar cell open-circuit voltage [9,10]. Temperature dependent photocurrent and dark measurements reveal that the primary cause for the reduction of the Voc is due

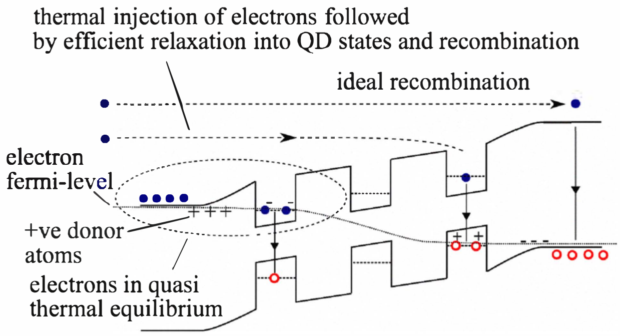

Fig. 8. The dominant dark current processes which lead to an increase of the dark current and a reduction of the open-circuit voltage.

to an increase of the dark current rather than an increase of the recombination of the photocarriers. The spectral response of the QDSC for a variety of temperatures is shown in Fig. 7 Also shown in the plot of Fig. 7. is the room temperature photoluminescence spectrum which can be compared to the spectral response to identify the locations of the QD and wetting layer response. At low temperature there is a strong bias dependent recombination of photocurrent. However, at room temperature the photo-generated carriers are readily thermally emitted from the QDs and collected as photocurrent and therefore the strength of room temperature photocurrent is a direct indication of the absorption strength of the QDs. For a QDSC to maintain a high Voc the QDs should not provide an additional dark current carrier recombination path with a smaller thermal activation energy. For that to be the case, carrier relaxation from barrier states to QD states should be inhibited. However, real QDSCs generally exhibit efficient dark current carrier relaxation and recombination from the QD ground state. Fig. 8 demonstrates the dominant dark current mechanisms of the QDSC. It can be concluded that there is currently still a lack of control over the thermal dynamics of QD charge carriers which prevents QD devices from obtaining optimal performance. In particular self-assembled QDs contain a large number of closely spaced energy levels and a band of wetting layer states. This deviation from an ideal QD which supports only a single excited energy level currently prevents QD devices from reaching a very high level of performance.

4. Conclusions

Semiconductor nanostructures have been successful in enhancing device performance where the improvements are due to changes in the thermal distribution of charge carriers. However, nanostructures have not been fully utilized to control electron-phonon interactions and therefore carrier thermal dynamics. This currently prevents QD devices such as QDIPs and QDSCs from achieving the theoretically predicted performance levels. Novel growth techniques and structures need to be developed to produce nanostructures with better engineered energy levels such that control over electron-phonon interactions is obtained.

Acknowledgement

Thanks are due to the Australian Research Council for the financial support of this research and the Australian National Fabrication Facility for access to facilities.

References

[1] J. S. Osinski, Y. Zou, P. Grodzinski, A. Mathur and P. D. Dapkus, "Low-threshold-current-density 1.5μm lasers using compressively strained InGaAsP quantum wells," Photonics Technology Letters, IEEE, **4**, 10-13 (1992).

[2] S. Shunji, and Y. Kiyoyuki; "Strain and quantum-confinement effects on differential gain of strained InGaAsP/InP quantum well lasers," J. Appl. Phys. **74**, 4242-4244 (1993).

[3] A. Rogalski, "Outlook on quantum dot infrared photodetectors," J. Opt. Memory and Neural Networks, **18**, 234-252 (2009).

[4] A. Marti, L. Cuadra, and A. Luque, "Partial filling of a quantum dot intermediate band for solar cells," IEEE Trans. Electron Devices, **48**, 2394-2399 (2001).

[5] N. Vukmirović, Ž. Gačević, Z. Ikonić, D. Indjin, P. Harrison and V. Milanović, "Intraband absorption in InAs/GaAs quantum dot infrared photodetectors - effective mass versus $k \times p$ modeling," Semicond. Sci. Technol. **21** 1098-1104 (2006).

[6] G. Jolley, L. Fu, H. H. Tan and C. Jagadish, "Properties of $In_{0.5}Ga_{0.5}As/GaAs/Al_{0.2}Ga_{0.8}As$ quantum-dots-in-a-well infrared photodetectors," J. Phys. D. **42**, 95101-95108 (2009).

[7] J.R. Andrews, S.R. Restaino, T.E. Vandervelde, J.S. Brown, Y.D. Sharma, S.J. Lee, S.W. Teare, A. Reisinger, M. Sundaram, and S. Krishna, "Comparison of Long-Wave Infrared Quantum-Dots-in-a-Well and Quantum-Well Focal Plane Arrays," IEEE Trans. Electron Devices, **56**, 512-516 (2009).

[8] D. Z. Y. Ting, S. V. Bandara, S. D. Gunapala, J. M. Mumolo, S. A. Keo, C. J. Hill, J. K. Liu, E. R. Blazejewski, S. B. Rafol, and Y. C. Chang, "Submonolayer quantum dot infrared photodetector," Appl. Phys. Lett. **94**, 111107-111109 (2009).

[9] G. Jolley, H. F. Lu, L. Fu, H. H. Tan, and C. Jagadish, "Electron-hole recombination properties of $In_{0.5}Ga_{0.5}As/GaAs$ quantum dot solar cells and the influence on the open circuit voltage," Appl. Phys. Lett. **97**, 123505-123505 (2010).

[10] H.F. Lu, L. Fu, G. Jolley, H.H. Tan, S.R. Tatavarti, C. Jagadish, "Temperature dependence of dark current properties of InGaAs/GaAs quantum dot solar cells," Appl. Phys. Lett. **98**,183509-183511 (2011).